Frontiers in Bioscience Landmark

Front. Biosci. (Landmark Ed) **2022**; 27(10): 296
https://doi.org/10.31083/j.fbl2710296

Original Research

The Role of the GRP78/PERK/ATF4 Pathway in the Ability of Gua Lou Gui Zhi Decoction to Attenuate Apoptosis by Inhibiting Endoplasmic Reticulum Stress after Ischemia-Reperfusion Injury

Yaping Chen[1,†], Zheming Chen[2,†], Weineng Cheng[1], Yajun Cao[1], Wen Xu[1], Wenfang Lai[1], Yuqin Zhang[1,*], Mei Huang[1,*], Lihong Nan[1,*]

[1]College of Pharmacy, Fujian University of Traditional Chinese Medicine, 350122 Fuzhou, Fujian, China
[2]Pharmaceutical Preparation Section, Quanzhou First Hospital, 362000 Quanzhou, Fujian, China
*Correspondence: 2016003@fjtcm.edu.cn (Yuqin Zhang); 2003002@fjtcm.edu.cn (Mei Huang); 2002017@fjtcm.edu.cn (Lihong Nan)
†These authors contributed equally.
Academic Editor: Taeg Kyu Kwon
Submitted: 14 June 2022 Revised: 12 September 2022 Accepted: 26 September 2022 Published: 31 October 2022

Abstract

Background: Endoplasmic reticulum stress (ERS) is a key part of the apoptotic cascade that is initiated after cerebral ischemia-reperfusion injury and is very important for research on poststroke rehabilitation. In addition, the unfolded protein response (UPR) plays an important role in ERS because it activates downstream apoptotic signal transduction and induces apoptosis through the glucose-regulated protein 78 (GRP78)/protein kinase R (PKR)-like ER kinase (PERK)/activating transcription factor 4 (ATF4) pathway. The Gua Lou Gui Zhi Decoction (GLGZD) ameliorated neuronal apoptosis of ischemia-reperfusion injury caused by middle cerebral artery occlusion (MCAO) had been proved in our previous study. The present study aims to underly the regulatory ability of GLGZD in ERS-induced apoptosis mediated by the GRP78/PERK/ATF4 pathway. **Methods**: GLGZD was analyzed by HPLC. The effects of GLGZD were obversed on MCAO-induced ischemic rats. The cerebral infarct volume was detected by 2,3,5-Triphenyl-2H-Tetrazolium Chloride (TTC) Staining. Terminal Deoxynucleotidyl Transferase-Mediated dUTP-Biotin Nick End Labeling (TUNEL) were used to detect apoptosis. Transmission Electron Microscopy (TEM), Ca^{2+} levels and reactive oxygen species (ROS) detection were used to determine the function of endoplasmic reticulum. The GRP78/PERK/ATF4 signaling pathway was assessed by western blotting and immunohistochemistry. **Results**: Our results showed that GLGZD exerted its effects on ischemia-reperfusion injury by significantly promoting the restoration of the quantity and morphology of the rough ER and reducing the neuronal apoptosis rate in the ischemic cortex. Moreover, both of the intracellular ROS and Ca^{2+} levels in ischemic cortical cells were found significantly reduced by GLGZD. The GLGZD-treated group showed increased levels of phosphorylation in both of PERK and eukaryotic translation initiation factor 2α (eIF2α), activation of cysteinyl aspartate-specific proteinase-3 (Caspase-3), upregulation of the total protein levels of sarcoplasmic/endoplasmic Ca^{2+} ATPase 2α (SERCA 2α) and B-cell leukemia/lymphoma gene 2 (Bcl-2). **Conclusions**: These findings suggest that GLGZD reduces oxidative stress-induced injury and promotes a dynamic calcium balance, thereby inhibiting ERS and exerting an antiapoptotic effect on neuronal ischemic injury, which are closely related to the activation of GRP78/PERK/ATF4 signaling pathway.

Keywords: cerebral ischemia-reperfusion injury; Gua Lou Gui Zhi Decoction; endoplasmic reticulum stress; GRP78/PERK/ATF4 pathway; neuronal apoptosis

1. Introduction

Stroke occurs abruptly, charactered with high morbidity, high mortality, and a high recurrence rate. There were ischemic stroke and hemorrhagic stroke on the basis of its pathogenesis. Ischemic stroke is more common, accounting for approximately 80% of all strokes, in which blood perfusion of the brain is altered, the dynamic equilibrium of ions is destroyed, and the metabolism of nerve cells is disrupted, ultimately inducing neuronal apoptosis and, in some cases, necrosis [1]. Approximately 70–80% of patients with stroke are plagued by limb motor dysfunction following stroke; among these defects, limb spasm has a high incidence rate and has become a major obstacle to patients' daily life and recovery [2]. Recent studies have indicated that the limb spasticity cause by stroke was related the loss control of upper motor neurons after ischemia, and the dissimilatory process in the superior spinal cord disappears. The inhibitory effect of the central nervous system on limb motor function is weakened, resulting in increased muscle tension. Cell apoptosis is the key cause of neuronal loss after stroke [3]. Therefore, in rehabilitation of stroke, one of the important therapy approaches is inhibiting ischemic neuronal apoptosis [4].

A variety of apoptosis studies have focused on mitochondria, and two intracellular apoptotic signaling pathways have been identified: the mitochondrial pathway and the death receptor pathway. According to recent studies, the mitochondria-associated endoplasmic reticulum (ER) couples with a variety of organelles in terms of structure and

function, conducted cell apoptosis through various pathways [5]. Changes in the intracellular environment is critical for the activation of ER. Both oxidative stress and Ca^{2+} overload caused by cerebral ischemia-reperfusion injury induce ER dysfunction, which is called endoplasmic reticulum stress (ERS) [6]. The unfolded protein response (UPR) is conducive to cell survival before stress exposure in ER. However, continual stress activates the downstream apoptotic pathway and induces apoptosis [7]. Activation of the glucose-regulated protein 78 (GRP78)/protein kinase R (PKR)-like ER kinase (PERK)/activating transcription factor 4 (ATF4) pathway is the main mechanism regulating UPR protein synthesis and maintenance of calcium ion equilibrium [8]. Therefore, the ERS pathway is a third intracellular signal transduction pathway mediating apoptosis, in addition to the mitochondrial and death receptor pathways, and provides a new therapeutic target for ischemic stroke treatment.

According to Traditional Chinese medicine recording, Gua Lou Gui Zhi Decoction (GLGZD) has been used in treating stroke and its sequelae for thousands of years. GLGZD is a classic formula in traditional Chinese medical work. In modern clinical practice, GLGZD is commonly used because of its efficacy in the treatment of limb spasm after stroke [9–11]. Our previous study established a high-performance liquid chromatography (HPLC) method to determinate the representative compounds in GLGZD [12,13]. The delegate chemical components of GLGZD have been qualitatively and quantitatively analyzed, and include citrulline, gallic acid, protocatechuic acid, paeoniflorin, glycyrrhizic acid, liquiritigenin, and isoliquiritigenin. These components are the foundation of GLGZD, they were reported had good effects in alleviating brain injury after cerebral ischemia-reperfusion. Based on these results, the treatment of GLGZD of ischemia-reperfusion injury mediated by the combined actions of these components. Furthermore, our previous works have suggested that GLGZD significantly inhibits neuronal apoptosis and exerts a neuroprotective effect *in vivo* and *in vitro* [13,14]. However, researchers have not reported whether the molecular mechanism of GLGZD is related to the regulation of ERS. Fistly, a suitable model of stroke was established in this study, we observed the therapeutic effects of GLGZD on ischemia-injured rats using middle cerebral artery occlusion (MCAO), and then further investigated whether GLGZD inhibits ischemic neuronal apoptosis through the GRP78/PERK/ATF4 signaling pathway activated by ERS, so as to clarify the mechanism of GLGZD on alleviating limb spasticity after stroke. Our findings provided a theoretical support for the efficacy of GLGZD in neurological rehabilitation after ischemic stroke.

2. Materials and Methods

2.1 Plant Material

Trichosanthis Radix, Cinnamomi Ramulu, Paeoniae Radix Alba, Glycyrrhizae Radix et Rhizoma, Jujubae Fructus and Zingiberis Rhizoma Recens were purchased from Beijing Tong Ren Tang Chinese Medicine Co., Ltd (Beijing, China). The mentioned Chinese medicinal materials were identified by Professor Yang Chengzhi from Fujian University of Traditional Chinese Medicine.

2.2 Animals

Seventy-five male Sprague-Dawley (SD) rats, weighing between 210 and 230 g, were purchased from purchased from Shanghai SLAC Laboratory Animal Co., Ltd. (license, SCXK (Hu) 2017–0005; Shanghai, China) and housed in the pathogen-free facility in the SPF animal experiment center of Fujian University of Traditional Chinese Medicine. Rats were maintained in a temperature-controlled facility at 22 $\pm$ 3 °C, under a 12 h light/dark cycle, and provided food and water ad libitum. The experiments began 7 days after adaptive feeding, which were done in accordance with the National Institutes of Health Guide for the Care and Use of Laboratory Animals, and the processes were approved by the Ethics Committee of Fujian University of Traditional Chinese Medicine (Fuzhou, China).

2.3 Preparation of GLGZD

Extraction of GLGZD was conducted according to the original composition recorded in the "Jin Kui Yao Lu". GLGZD was made up with 30 g of Trichosanthis Radix, 9 g of Cinnamomi Ramulu, 9 g of Paeoniae Radix Alba, 6 g of Zingiberis Rhizoma Recens, 9 g of Jujubae Fructus, and 6 g of Glycyrrhizae Radix et Rhizoma. These medicinal materials were crushed, sequentially extracted with 10 and 8 volumes of ddH_2O with refluxing for 1.5 h, and then filtered. The filtered extract fractions were collected, combined, and concentrated the final concentration of GLGZD to 1.44 $g{\cdot}mL^{-1}$. The quality control procedure used to confirm that GLGZD has been previously established and described [12,13], and the main components of GLGZD fingerprint was analyzed by the HPLC (Fig. 1).

2.4 Establishment of the MCAO Model

The model of MCAO was conducted by an intraluminal block, as we usually do [13]. Firstly, anesthetized the rats by intraperitoneal injection of 2% sodium pentobarbital (60 mg/kg), and then inserted a 3–0 silicon rubber-coated nylon monofilamen into the internal carotid artery (ICA) (about 18 mm from the CCA bifurcation). The filament was partially removed (~1.5 cm) for reperfusion after embolization for 2 h. After modeling, all rats were transferred to a clean cage and kept warm. When rats were awake, neurological function was scored using the Zea Longa scale

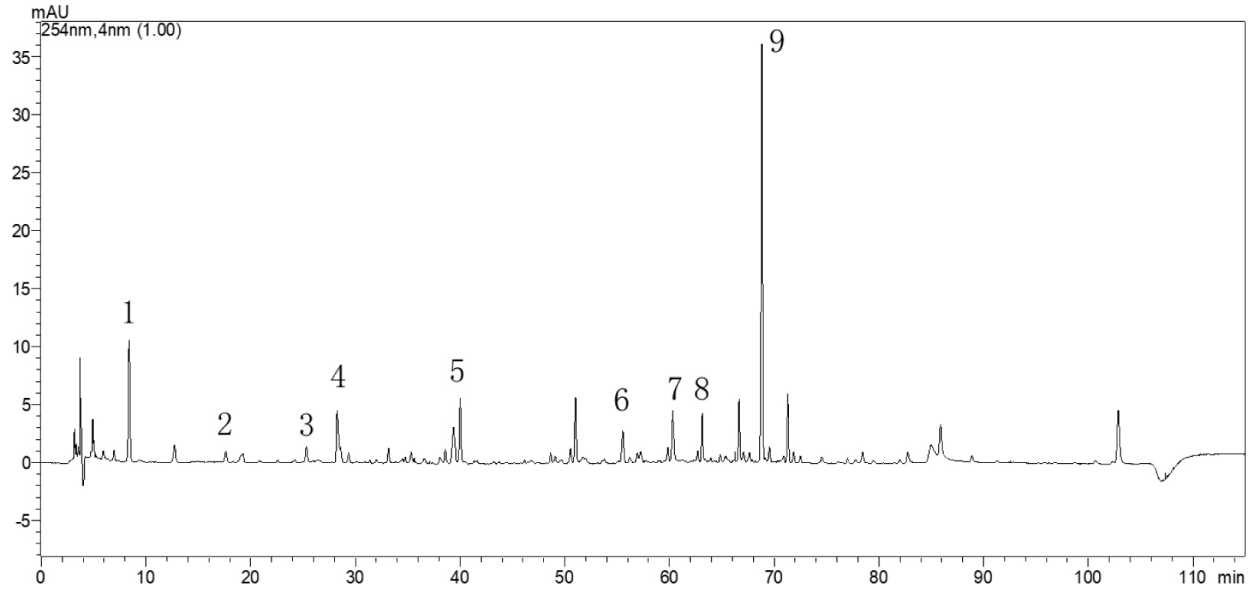

Fig. 1. Fingerprint of the GLGZD. 1, gallic acid; 2, protocatechuic acid; 3, albiflorin; 4, paeoniflorin; 5, glycyrrhizin; 6, liquiritigenin; 7, cinnamic acid; 8, cinnamaldehyde; and 9, glycyrrhizic acid.

[15], and muscle tension was determined using the modified Ashworth method [16]. The scoring processes were performed by two experimenters who were familiar with the scoring criteria but not participated in the experiments, they completed scoring simultaneously and independently in a double-blind manner. A higher score indicates greater nerve injury severity.

Only rats with limb paralysis and neurological function scores of 2 to 4 were included in subsequent experiments. The total number male SD rats were seventy-five, of them twelve rats were randomly assigned for the sham operation, and the remaining rats were used as the operation group. Five rats in the operation group had no neurological deficits or muscular hypertonia and were subsequently excluded from the experiment, and nine rats died during the experimental procedures. The rest forty-nine rats were successfully modeled rats.

2.5 Groups and Administration

Rats that were successfully modeled assigned randomly into four groups after MCAO modeling (n = 12). The rats in the MCAO group were administered saline. Rats in the GLGZD low-dose group (GLGZD-L) were administered GLGZD at the concentration of 0.36 g·mL^{-1}. Rats in the GLGZD middle-dose group (GLGZD-M) were administered GLGZD at the concentration of 0.72 g·mL^{-1}. Rats in the GLGZD high-dose group (GLGZD-H) were administered GLGZD at the concentration of 1.44 g·mL^{-1}. In the sham operation process, there was no suture inserted in the sham group, the other surgical operations were the same as the MCAO groups. Besides, the sham rats were administered a volume of saline equal to that of other treatments daily after the sham operation. All the aforementioned regimens were administered 10 mL/kg, once a day for 7 days, the administration by gavage began after grouping on the day of the operation. The therapeutic effects of GLGZD were observed by the changes in nerve function, muscle tension, cerebral infarct volume, and the pathological state of the ischemic cerebral cortex in MCAO rats. For details, please refer to our previous study [13].

2.6 Motor Function Test

The CatWalk test is a sensitive and reliable method to detect motor function deficits in rats. One week before the test, the rats in this study were trained to pass a Catwalk channel smoothly in 10 s in a dark room environment. The movement of the rat was evaluated using CatWalk gait analysis (XT10.0, Noldus Information Technology Co., Ltd., Wageningen, The Netherlands) 1 h after the last treatment was administered. During the measurement, footprint refraction technology with an internal light source was used to perform efficient computer processing of the footprints recorded by video, and hence, the gait parameters of each mouse were evaluated.

2.7 2,3,5-Triphenyl-2H-Tetrazolium Chloride (TTC) Staining

The brains were excised rapidly after rats were decapitate. The brain parenchyma (after discarding the olfactory bulb, cerebellum and lower brain stem) was precooled with a –20 °C refrigerator for 5 min, and cut into 2-mm slices using stainless steel brain matrices. The slices were incubated in a closed container with TTC solution (Sigma, St. Louis, MO, USA) at 37 °C for 30 min in the dark, during incubation flipped sections every 10 min for evenly dyed. Images of cerebral infarct were captured with a digital cam-

era (Nikon, Tokyo, Japan). Infarct volume of each section was traced and calculated using Image-Pro Plus 6.0 software (Media Cybernetics, Rockville, MD, USA).

2.8 Terminal Deoxynucleotidyl Transferase-Mediated dUTP-Biotin Nick End Labeling (TUNEL) Assay

Rats were anesthetized after the last administration. The thorax was opened and a perfusion needle was fixed on the left ventricle via the apex of the heart, and a small opening in the right atrial appendage was cut for perfusion. Then, mice were successively perfused with ice-cold saline and fixative containing 4% paraformaldehyde (PFA)/PBS. Brain tissues were excised for another 24 h fixing, and subsequently embedded. The paraffin-embedded brains were cut into 4 μm slices and mounted on a glass slide. The sections were dewaxed to water, incubated with diluted proteinase K solution (10 min at room temperature) after fixed with 4% PFA (5 min). Subsequently, the slices need another fix with 4% PFA for 5 min, and then equilibration buffer was added for 10-min equilibration. And then added TdT enzyme reaction solution (Promega, Madison, WI, USA) for an incubation in the dark for 1 h in a humidified chamber at 37 °C. 2$\times$ sodium citrate buffer was added after the reaction was terminated. Next, dyed the nuclei with DAPI dye solution (Beyotime Biotechnology, Beijing, China). The stained sections were sealed and captured the images under a laser confocal microscope (Leica, Wetzlar, Germany). The intensity of TUNEL staining cells was analyzed using Image-Pro Plus 6.0 software. The TUNEL-positive rate was calculated by (TUNEL-positive cells/nuclear DAPI-positive cells) $\times$ 100%.

2.9 Transmission Electron Microscopy (TEM)

Rat cerebral tissue in a volume of 1 mm $\times$ 1 mm $\times$ 1 mm was fixed using the electron microscopy fixative solution (Servicebio Technology Co., Ltd., Wuhan, China) at 4 °C for 4 h. In addition, the sample was washed with PBS for 3 $\times$ 15 min. The sample was conventionally dehydrated and gradually embedded, incubated overnight at 37 °C in an embedding plate, and cured at 60 °C for 48 h. The polymerized tissue samples were sectioned into 60 nm ultrathin microsections and sequentially stained with 2% uranyl acetate and lead citrate both for 15 min. Dried them overnight at room temperature. Pathological changes in the ER were obtained with a transmission electron microscope (Hitachi, Tokyo, Japan).

2.10 Immunohistochemistry

Paraffin sections (4 μm) were conventionally dewaxed, 3% H_2O_2 was added to the surface of the sliced tissue for 15-min incubation. For antigen retrieval, the sections were boiled for 15 min in boiling sodium citrate buffer. 5% bovine serum albumin (BSA) was used to blocked non-specific binding. Then, the rabbit polyclonal anti-IP3R antibody (1:500, Abcam, Cambridge, UK) was added for incubation overnight at 4 °C. Twenty-four hours later, covered the slides with biotin-labeled goat anti-rabbit IgG (1:500, Thermo Fisher Scientific, Waltham, MA, USA) for another incubation at room temperature in the dark for 2 h. Horseradish peroxidase (HRP)-streptavidin conjugate (SABC) solution (Boster Biological Technology, Wuhan, China) was dropped to the tissue slices and stayed for 30 min. And then, the tissue slices were stained with 3,3′-diaminobenzidine (DAB) color development kit (Boster Biological Technology, Wuhan, China) and hematoxylin. The slice was covered, and images were captured at a magnification of 400$\times$ under a laser confocal microscope. The positive cells were counted in 5 different parts of each slice and analyzed by Image-Pro Plus 6.0.

2.11 Immunofluorescence Staining

Paraffin sections (4 μm) were routinely dewaxed and antigens were retrieved. For immunofluorescence staining, the sections were washed with PBS, and followed by 5% BSA blocking at room temperature for 2 h. Subsequently, the sections were incubated overnight with a primary rabbit polyclonal anti-GRP78 antibody (1:500, Bioworld Technology, MN, USA) at 4 °C. Twenty-four hours later, the sections were washed with PBS. And then a fluorescent goat anti-rabbit IgG secondary antibody (1:200, Abcam, Cambridge, UK) was incubated for 2 h (protect from light). 40 μL anti-quenching agent was added after the nuclei were stained with DAPI solution for 7 min, and then covered the slices. The images were captured at a magnification of 200$\times$ by a fluorescence microscope (Leica, Wetzlar, Germany). The positive cells in 5 different parts of each slice were analyzed by Image-Pro Plus 6.0.

2.12 Fluorescent Probe

The ischemic cerebral cortex was isolated from the excised brains. 0.25% trypsin was added in two hundred micrograms of tissue for digestion under a 37 °C-water bath for 30 min. Three volumes of precooled PBS were added to terminate digestion. Collected the cell suspension and filtered through a 300-mesh nylon filter. The filtrate was centrifuged at 500 $\times$ g and the supernatant was discarded, the cells were resuspended with PBS at a density of 10^6 cells·mL^{-1}. Fluorescent probes were added to the sample solution; both calcium fluorescent probes (Beyotime Biotechnology, Shanghai, China) and reactive oxygen species (ROS) fluorescent probes were prepared. After incubation for 1 h at 37 °C, the samples were centrifuged at

1000 × *g* for 10 min, and collected the precipitate for probe detection. The calcium concentration was detected with a microplate reader multiwavelength measurement system (TECAN, Männedorf, CH) at an excitation wavelength of 488 nm and an emission wavelength of 505 nm. ROS levels were measured with the same microplate reader at an excitation wavelength of 488 nm and emission wavelength of 525 nm. The bicinchoninic acid (BCA) assay (Beyotime Biotechnology, Shanghai, China) was used to measure the total protein. Intracellular ROS levels and Ca^{2+} concentrations were assessed and are reported with respect to total protein concentration as arbitrary intensity/total protein concentration.

2.13 Isolation of Total Proteins and Nucleoproteins

The brain was quickly excised after rats were sacrificed, and the ischemic cortex was isolated. The cortex samples were ground to a powder with liquid nitrogen.

For total proteins extraction, every one hundred milligrams of the tissue powder were lysed by 1 mL of RIPA lysis buffer (Beyotime Biotechnology, Shanghai, China) on ice bath for 30 min. Lysates were centrifuged at 14,000 rpm for 30 min at 4 °C. Collected the supernatant to obtain total protein.

For nucleoproteins extraction, every One hundred milligrams of the tissue powder were added in 1 mL of cytosolic extraction reagent (Beyotime Biotechnology, Shanghai, China) and the sample was placed on ice for 20 min. Then centrifuged the extraction of samples at 14,000 × *g* for 10 min at 4 °C. Carefully discard the supernatant, and added 200 μL of the nuclear extraction reagent (Beyotime Biotechnology, Shanghai, China), mixed thoroughly by vortexing. Then centrifuged the samples at 14,000 × *g* for 10 min at 4 °C after another 30-min ice bath. Collected the supernatant to obtain the nucleoprotein.

2.14 Western Blot Analysis

The proteins concentrations were obtained by the BCA method after extracting protein from each sample lysate. Then the protein sample was added loading buffer and boilled at 100 °C for 10 min-denaturation. Proteins (50 μg) were separated by 10% sodium dodecyl sulfate-polyacrylamide gel electrophoresis (SDS-PAGE), then electro-transferred to a nitrocellulose (NC) membrane. 5% skim milk in Tris-buffered saline containing 0.1% Tween-20 (T-TBS) was used for blocking for 2 h. Then probed with the indicated primary antibodies rabbit polyclonal anti-GRP78 antibody (1:1000, Bioworld Technology, Minneapolis, MN, USA) , rabbit polyclonal anti- cysteinyl aspartate-specific proteinase-3 (Caspase-3) antibody, monoclonal anti-PERK-rabbit antibody, rabbit monoclonal anti-phosphorylated (p)-PERK antibody (1:1000, Cell Signaling Technology, Boston, MA, USA), mouse monoclonal anti-eukaryotic translation initiation factor 2α (eIF2α) antibody, rabbit monoclonal anti-p-eIF2α antibody (1:1000, Cell Signaling Technology, Boston, MA, USA), rabbit monoclonal anti-ATF4 antibody (1:1000, Abcam, Cambridge, UK), rabbit monoclonal anti-C/EBP homology protein (CHOP) antibody (1:1000, Abcam, Cambridge, UK), rabbit monoclonal anti-endoplasmic reticulum oxide 1α (Ero-1α) antibody, rabbit monoclonal anti-Bcl-2 antibody, rabbit monoclonal anti-Bax antibody (1:1000, Abcam, Cambridge, UK), mouse monoclonal anti-β-actin antibody, mouse monoclonal anti-histone H3 antibody (1:1000, Beyotime Biotechnology, Shanghai, China) and rabbit polyclonal anti-cleaved Caspase-3 antibody (1:500, Cell Signaling Technology, Boston, MA, USA)) overnight at 4 °C. The next day, after rinsing with TBST, the following HRP-linked secondary antibodies were added: goat anti-mouse IgG and goat anti-rabbit IgG (1:1000, Thermo Fisher Scientific, Waltham, MA, USA). The enhanced chemiluminescence (ECL) kit (Beyotime Biotechnology, Shanghai, China) was applied to visualize immunoblot signals after rinsing, and the protein signal was detected with the Chemi-Doc MP system (Bio-Rad, CA, USA). Density value of bands was quantitatively analyzed by Image Lab 4.1 software (Bio-Rad Laboratories, Hercules, CA, USA). The internal standard for total proteins was β-Actin. The internal standard for nucleoproteins was Histone H3. The expression level of the target protein = the gray value of target band/the gray value of the internal band.

2.15 Statistical Analysis

Data obtained were statistically analyzed with SPSS software, version 20.0 (SPSS, Inc., Chicago, IL, USA), and presented as the means ± SD. The neurological deficit score and the muscle tension score were analyzed by using the Kruskal-Wallis test. The rest data were statistically analyzed one-way ANOVA. The LSD test was used to compare data with a normal distribution and homogeneity of variance, otherwise the Games-Howell test was applied. *p*-values below 0.05 were defined as statistically significant.

3. Results

3.1 Quality Control of GLGZD Using HPLC

The chromatographic fingerprint was acquired by qualitative and quantitative HPLC analysis (Fig. 1). In the extraction of GLGZD, 9 main compounds including gallic acid, protocatechuic acid, albiflorin, paeoniflorin, glycyrrhizin, liquiritigenin, cinnamic acid, cinnamaldehyde and glycyrrhizic acid were detected.

3.2 GLGZD Alleviates Nerve Function Damage, Muscle Tension and Cerebral Infarct Volume in MCAO-Injured Rats

Neurological deficits of the MCAO-injured rats were assessed using Longa's method, and muscle tension was scored with the modified Ashworth scale on days 1, 3, 5 and 7 after modeling. Compared with the sham group, there were significant increases of the neurological func-

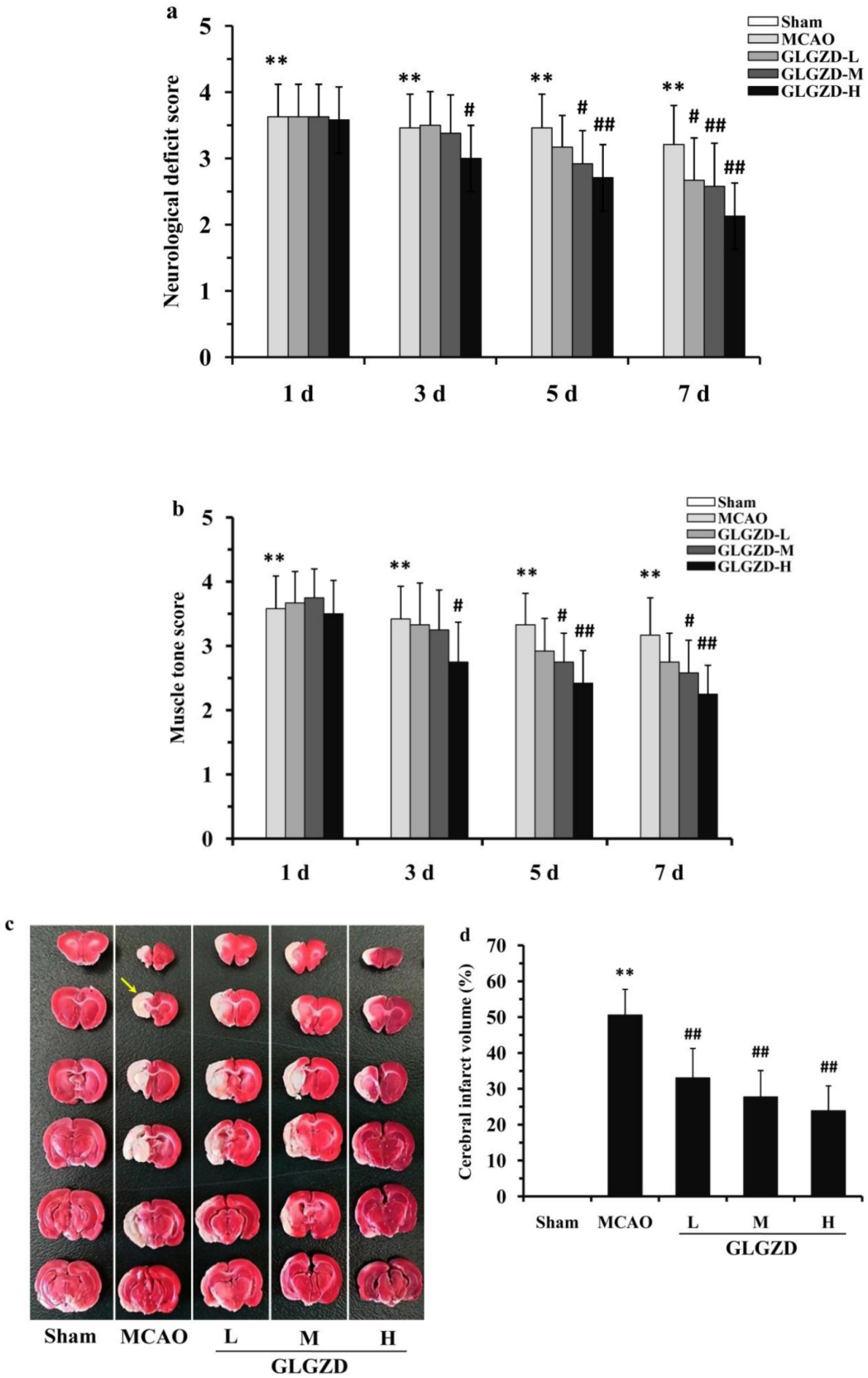

Fig. 2. GLGZD alleviates neurological deficits, muscle tension and the cerebral infarct volume in MCAO-injured rats. (a) Neurological function scores. (b) Muscle tension scores. (c) Representative images of TTC-stained cerebral slices, yellow arrows indicated the "infarct zone". (d) Quantitative analysis of the cerebral infarct volume. All data are presented as the means ± SDs. $^{**}p < 0.01$ compared with the sham group; $^{\#}p < 0.05$ and $^{\#\#}p < 0.01$ compared with the MCAO group.

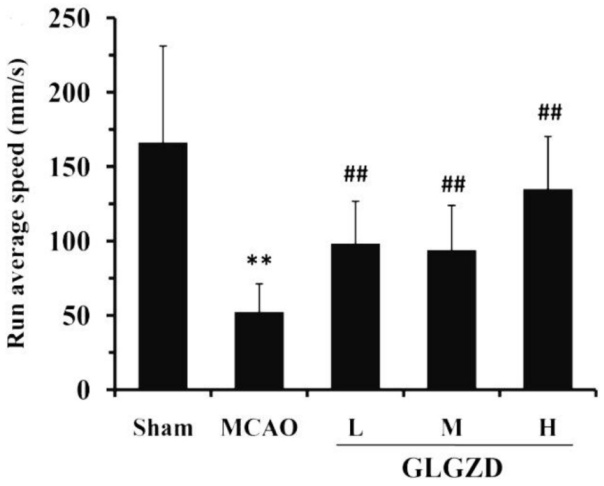

Fig. 3. GLGZD improves the motor function of rats after MCAO. The CatWalk gait analysis system indicates the limb motor function of rats by measuring the gait parameters. The CatWalk gait analysis system was used to quantitatively assess the average running speed of the rats, indicating the limb motor function of the rats. All data are presented as the means ± SDs. $^{**}p < 0.01$ compared with the sham group; $^{\#\#}p < 0.01$ compared with the MCAO group.

tion score, muscle tension score and cerebral infarct volume in the MCAO group ($p < 0.01$) (Fig. 2a–d). Additionally, the TTC staining slices in the sham group were observed rose-carmine, identified no infarction. There was no staining in the MCAO group slices and appeared to be white, which was identified cerebral infarct area, indicated that the cerebral infarct volume was significantly increased after MCAO modeling ($p < 0.01$). These data suggested that the MCAO model was successfully constructed. After GLGZD administration, the neurological deficit and muscle tension of GLGZD-H group were significantly alleviated on days 3, 5 and 7 ($p < 0.05, p < 0.01$). And the scores in GLGZD-M group were significantly reduced on days 5 and 7 ($p < 0.05$, $p < 0.01$). Furthermore, after 7 days' GLGZD administration, the cerebral infarct volume reduced significantly ($p < 0.01$).

3.3 GLGZD Improves the Motor Function in MCAO-Injured Rats

Results in Fig. 3 indicated that paralysis of the right front limbs of the MCAO rats was obvious after cerebral ischemia reperfusion injury. It was found the average running speed of MCAO rats was significantly decreased after surgical operation ($p < 0.01$). However, 7 days treatment of GLGZD significantly ameliorated the disordered motor function in MCAO modeling rats ($p < 0.05, p < 0.01$).

3.4 GLGZD Inhibits Cell Apoptosis in the Ischemic Rat Cerebral Cortex of the MCAO Model

Based on observations of TUNEL staining (Fig. 4a,b), compared with the sham operation group, the TUNEL-positive cells in the cortex of MCAO rats were found significantly increased ($p < 0.01$). The intragastric administration of GLGZD for 7 days displayed significantly downregulated on the number of apoptotic cells ($p < 0.05, p < 0.01$).

3.5 GLGZD Ameliorates ER Morphology in the Ischemic Rat Cerebral Cortex of the MCAO Model

TEM images are displayed in Fig. 5. The nuclear membrane structure of the sham group was clear and complete, rough ER was abundant. In addition, the cell arrangement was neat and concentric. The ER of the MCAO group was significantly decreased and disordered. The ER structure was altered, and expansion, swelling, and vacuolization were apparent. However, the structure and function of the rough ER were significantly ameliorated after GLGZD treatment, and the number of rough ER was predominantly upregulated ($p < 0.05, p < 0.01$).

3.6 The Ca^{2+} Concentration and ROS Levels in the Cells of the Ischemic Rat Cerebral Cortex of the MCAO Model Aggravated by GLGZD Treatment

The results obtained with the fluorescence probe are shown in Fig. 6a,b, they indicated that the Ca^{2+} concentration and ROS levels in cells of the MCAO-injured rats cortex increased significantly ($p < 0.01$) compared with the sham operation group. GLGZD administration significantly reduced ROS levels and the concentration of Ca^{2+} in the cells of the ischemic rat cerebral cortex ($p < 0.05, p < 0.01$).

3.7 IP3R Expression in the Ischemic Areas of the Brains of MCAO-Injured Rats Attenuated by GLGZD Treatment

Immunohistochemistry staining (Fig. 7a,b) demonstrated that the IP3R, a protein mainly located in the nucleus and cytoplasm, increased significantly in the ischemic cortex of the MCAO group compared with the sham operation group ($p < 0.01$). Interestingly, the expression of IP3R protein in the ischemic cortex downregulated significantly by GLGZD treatment ($p < 0.05, p < 0.01$).

3.8 GLGZD on GRP78, PERK, p-PERK, eIF2α, p-eIF2α, CHOP, Bcl-2, Caspase-3, cleaved Caspase-3, Ero-1α, SERCA 2α, Bax and ATF4 Protein Levels of the MCAO Modeling Ischemic Rat Cerebral Cortex Regulated by GLGZD Treatment

Western blot analyse are shown in Fig. 8a–f, the levels of the total GRP78, ATF4, CHOP, Ero-1α and Bax proteins in the ischemic rat cortex of the MCAO group were significantly increased compared with the sham group ($p < 0.01$). In contrast, the levels of the total Bcl-2 and sarcoplasmic/endoplasmic Ca^{2+} ATPase 2α (SERCA 2α) was

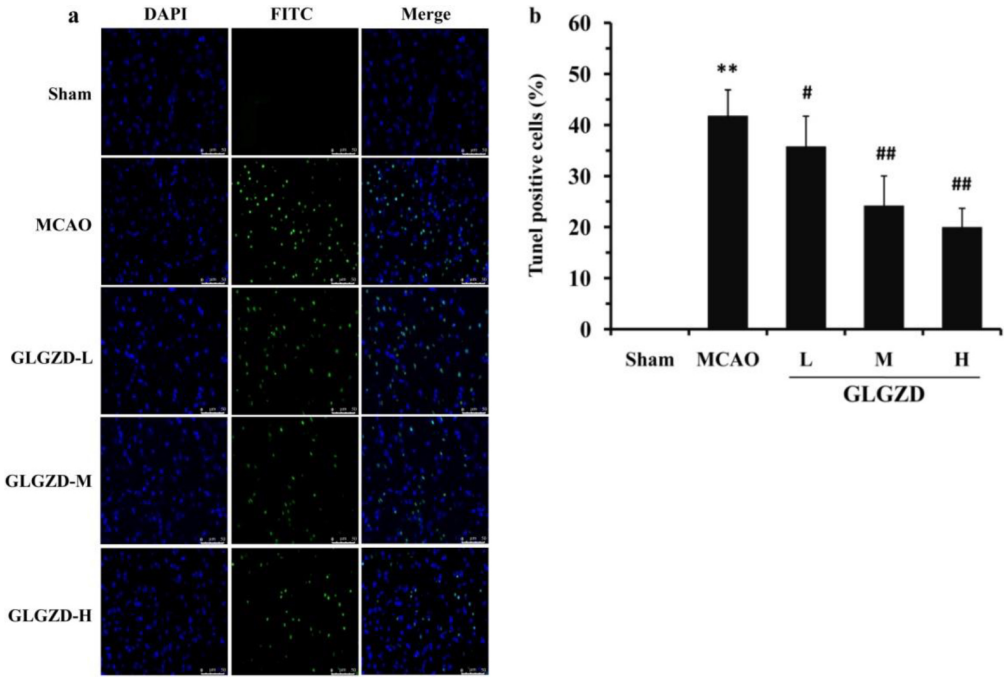

Fig. 4. GLGZD inhibits cell apoptosis in the ischemic cerebral cortex of the rats after MCAO. The 3'-carboxy terminus is exposed when DNA is damaged, and thus fragmented DNA in apoptotic cells exhibits green fluorescence after TUNEL staining. The nuclei of the cells presented blue fluorescence after DAPI staining. Only the cells labeled with both of these fluorescence stains were considered positive cells. (a) Representative morphology of the apoptotic cells (400×) determined using laser confocal microscopy after TUNEL staining. (b) Quantitative analysis of TUNEL-positive cells. All data are presented as the means ± SDs. $^{**}p < 0.01$ compared with the sham group; $^{\#}p < 0.05$ and $^{\#\#}p < 0.01$ compared with the MCAO group.

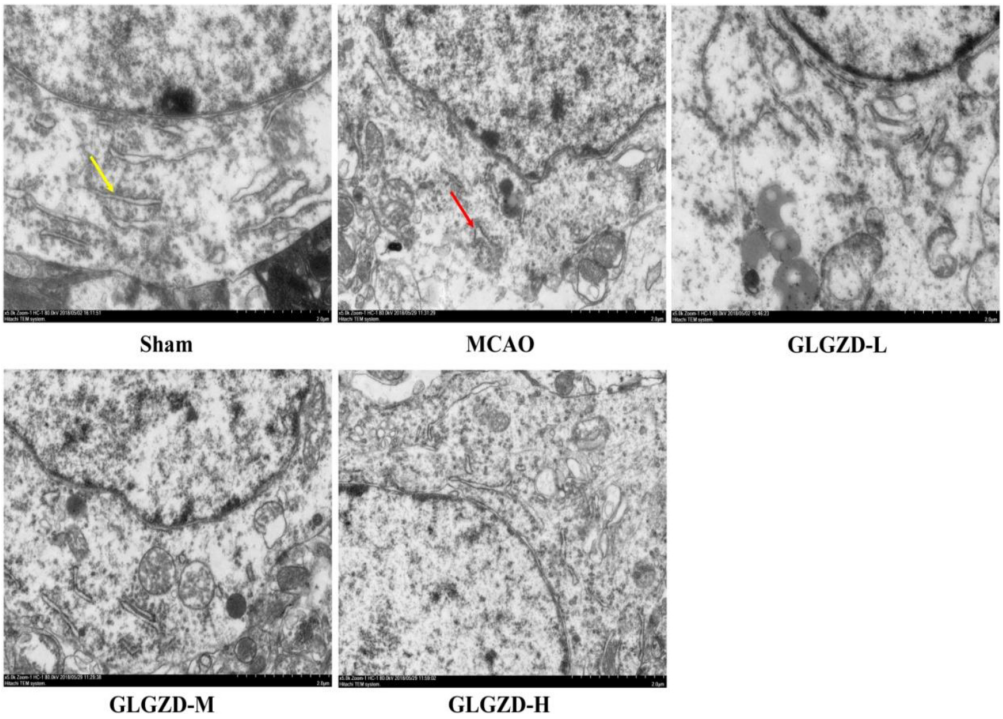

Fig. 5. ER morphology in the ischemic cerebral cortex of MCAO-injured rats viewed using TEM; (10000×). The yellow arrowhead indicates the rough ER in the cerebral cortex of the sham group of rats with a normal shape, complete structure and rolled-up concentric ring-like figures. The red arrowhead indicates representative synapses. The rough ER in the cerebral cortex of the MCAO group of rats showed various pathological changes, including expansion, swelling, vacuolization, a disordered arrangement and a blurry outline.

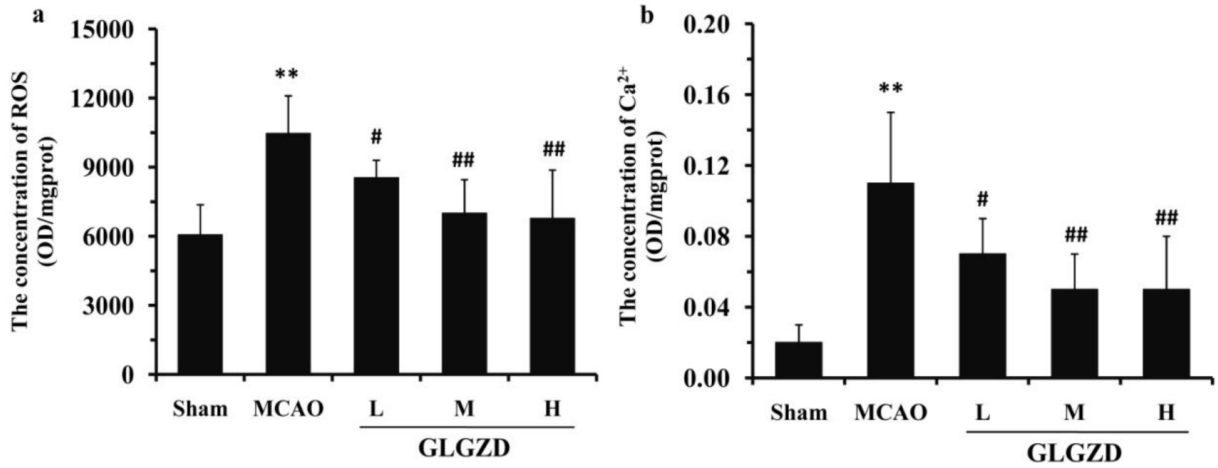

Fig. 6. Effects of GLGZD on the Ca^{2+} concentration and ROS levels in cells in the ischemic cerebral cortex of MCAO-injured rats (as determined with the fluorescence probe method). ROS levels (a) and Ca^{2+} concentration (b) in all groups. All data are presented as the means ± SDs. $^{**}p < 0.01$ compared with the sham group; $^{\#}p < 0.05$ and $^{\#\#}p < 0.01$ compared with the MCAO group.

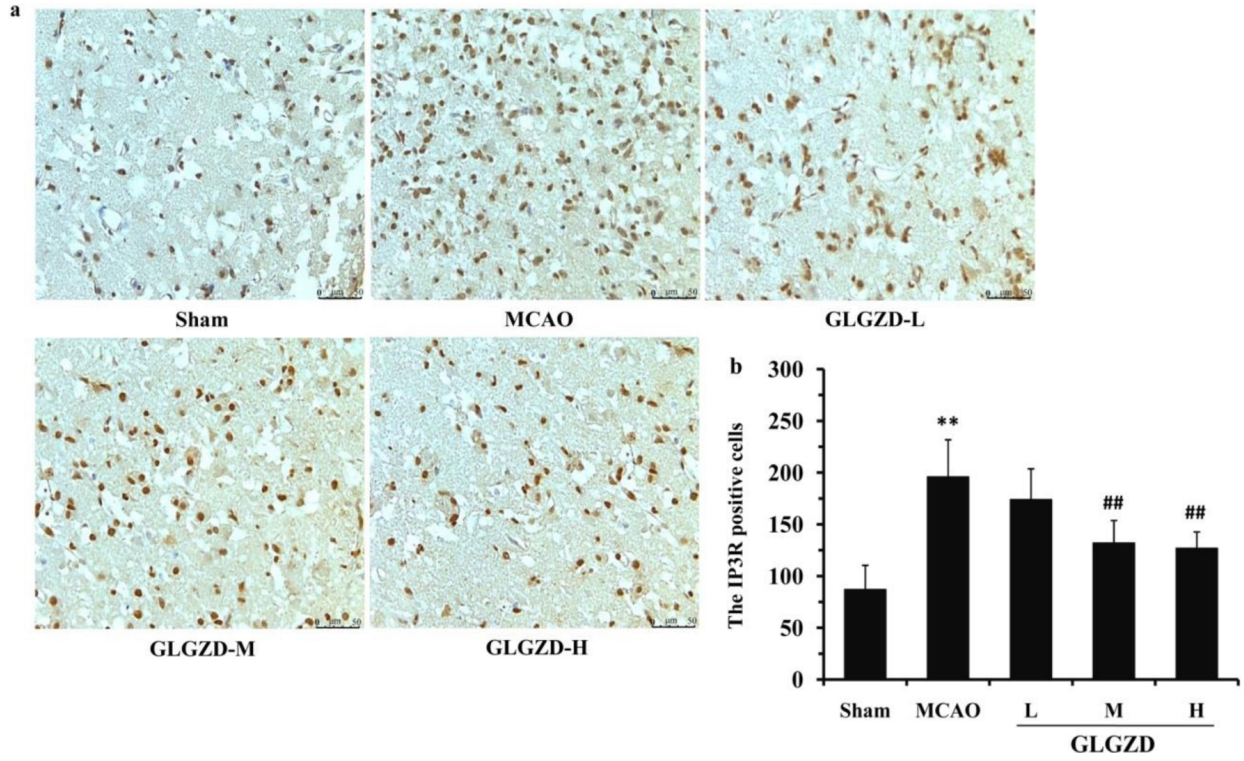

Fig. 7. Effects of GLGZD on the expression of the IP3R protein in the ischemic area of the rats after MCAO. (a) The IP3R protein was stained using immunohistochemical method, with the positively stained protein appearing brown. The expression and location of IP3R were observed using electron microscopy (400×). (b) Analysis of the relative optical density analysis of IP3R expressed in the cerebral cortex. All data are presented as the means ± SDs. $^{**}p < 0.01$ compared with the sham group; $^{\#}p < 0.05$ and $^{\#\#}p < 0.01$ compared with the MCAO group.

significantly reduced ($p < 0.01$). The protein levels of GRP78, ATF4, CHOP, Ero-1α, and Bax of the GLGZD-H and GLGZD-M groups significantly decreased, at the same time, Bcl-2 and SERCA 2α levels in the GLGZD-M group ($p < 0.05$, $p < 0.01$) significantly increased.

As shown in Fig. 8g,h, compared the MCAO group with the sham group, a significant increase of the phosphorylated form of PERK and EIF2α proteins were found in the cortex of rat ($p < 0.05$, $p < 0.01$). Interestingly, GLGZD also significantly reversed the phosphorylation in a dose-dependent manner ($p < 0.05$, $p < 0.01$).

As shown in Fig. 8i,j, compared the MCAO group

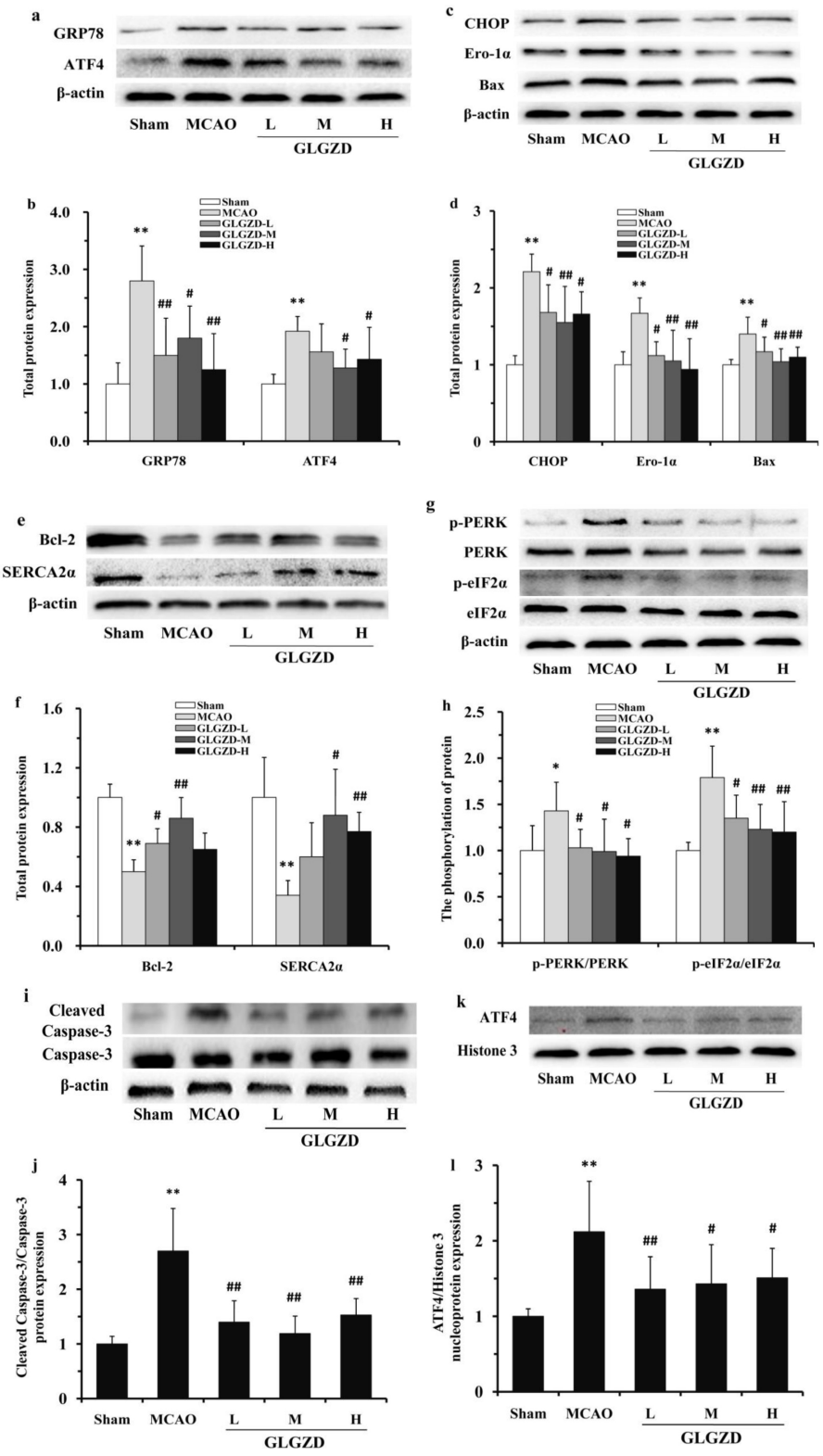

Fig. 8. Effects of GLGZD on the expression of proteins in the PERK/ATF4 signaling pathway-related the ischemic cortex of the rats after MCAO. Representative Western blots (a), (c), (e) and the relative optical densities (b), (d), (f) of the total protein levels of GRP78, ATF4, CHOP, Ero-1α, Bax, Bcl-2 and SERCA 2α. The internal standard for total protein was β-Actin. Representative Western blot (g) and the relative optical densities (h) of the levels of phosphorylated PERK and eIF2α. Representative Western blot (i) and relative optical density (j) of the level of activated Caspaedse-3. Representative Western blot (k) and relative optical density (l) of the expression of the nucleoprotein ATF4. The internal standard for nucleoprotein was Histone H3. All data are presented as the means $\pm$ SDs. *$p <$ 0.05 and **$p < 0.01$ compared with the sham group; $^{\#}p < 0.05$ and $^{\#\#}p < 0.01$ compared with the MCAO group.

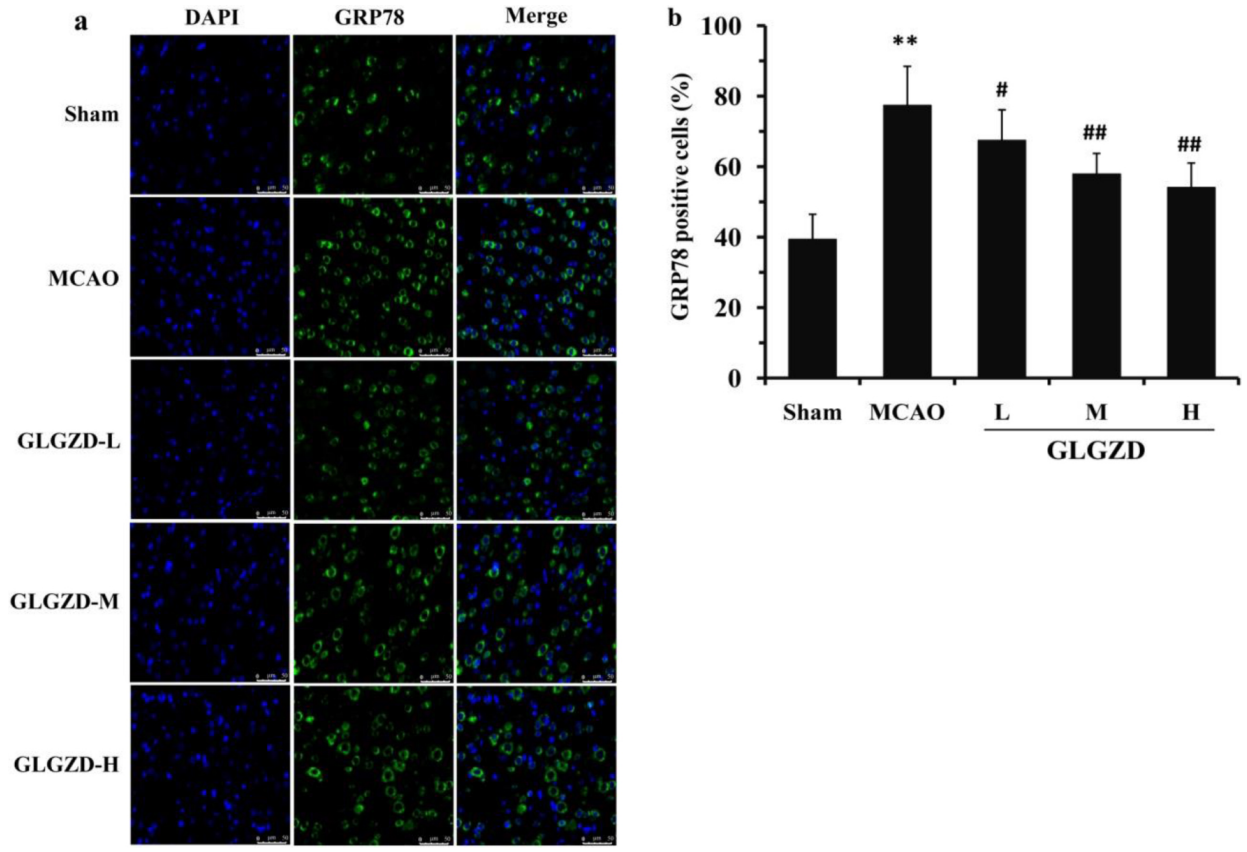

Fig. 9. Effects of GLGZD on GRP78 protein expression of in the ischemic cortex of rats after MCAO. (a) Immunofluorescence staining showing the location and expression of the GRP78 protein (400×). The nucleus is stained blue with DAPI, GRP78 is labeled in green, and positive cells are shown in the superposition of the two images. (b) Analysis of GRP78-positive cells. All data are presented as the means ± SDs. $^{*}p < 0.05$ and $^{**}p < 0.01$ compared with the sham group; $^{\#}p < 0.05$ and $^{\#\#}p < 0.01$ compared with the MCAO group.

with the sham group, the level of cleaved caspase-3, a marker of apoptosis, was significantly increased in the ischemic cortex of rat ($p < 0.01$). GLGZD effectively decreased the level of activated Caspase-3 in all treatment groups ($p < 0.01$).

As shown in Fig. 8k,l, compared the MCAO group with the sham group, the nuclear expression of ATF4 was significantly increased in the ischemic cortex of rat. After 7 days administration of GLGZD, the nucleoprotein ATF4 expressed level in ischemic cortex was significantly lower than that in the MCAO group ($p < 0.05$, $p < 0.01$).

3.9 Immunofluorescence Labeling of GRP78 Protein Expression in the Ischemic Cortex of MCAO-Injured Rats Attenuated by GLGZD Treatment

Immunofluorescence staining (Fig. 9a,b) showed that the GRP78 was mainly located in the cytoplasm. The ischemic cortex of the MCAO group had a significantly higher expression of GRP78 than that of the sham group ($p < 0.01$). The GRP78 protein expressed in the cytoplasm was significantly reduced by GLGZD treatment ($p < 0.05$, $p < 0.01$).

4. Discussion

The blood supply zone in middle cerebral artery is a core region affected by ischemic cerebrovascular disease. Hence, A MCAO model was established, by inserting a standard microballoon catheter intraluminally from the common carotid artery into the middle cerebral artery proximal segment, to mimick clinical cerebral ischemic diseases [17]. Neurological deficits were assessed by calculating neurological function scores typically used as scoring standards in scientific analyses. The method we used is one of the most widely used methods for judging whether a MCAO model has been successfully established in experimental research [18]. Longa's 5-point scoring system is recognized as one of the scoring standards of neurological function. The upper motor neuron injury after cerebral ischemia led to limb spasticity, which is a motor dysfunction after stroke. The spasticity is followed by excitability of motor circuits and an increase in muscle tension in limbs [4]. Therefore, muscle tension was assessed with the modified Ashworth scale, which was also used to indirectly indicate the limb spasticity of the rats.

In our experiment, when blocking the middle cerebral artery of the MCAO rats by a thread plug, neurological

deficits in the rats were observed. For example, rats fell to the opposite side when walking, and some rats cannot walk without assistance. The MCAO operation significantly increased the muscle tension score and cerebral infarct volume. The muscle tension scores were all >1. It turned out clearly that the MCAO model was successfully constructed. One of the most obvious features of limb motor dysfunction after cerebral ischemia is Abnormal gait, and it is also one of the external manifestations of nerve function injury. Accordingly, the motor function of rats was quantitatively analyzed using a Catwalk gait analysis system in this study. The results of the Catwalk analysis quantitatively revealed the motor function changes in the rats: The average running speed of the MCAO-injured rats was significantly lower than sham group of rats ($p < 0.01$). These results support the idea that the motor function significantly reduced due to the cerebral ischemia injury. Surprisingly, treatment with GLGZD for 7 days significantly decreased the muscle tension scores, neurological function scores and cerebral infarct volumes of the ischemia-injured rats ($p < 0.05$, $p < 0.01$).

Apoptosis was reported the main type of cell death caused by ischemia-reperfusion injury in the ischemic penumbra cortex, it is the culmination of a programmed cell death process controlled by genes. Apoptosis in ischemia-reperfusion injury is intimately involved in the development and expansion of cerebral infarction [19]. In our study, the neurons showed a relatively complete cellular architecture and potential metabolic capability, indicating that the apoptosis process in the MCAO model was reversible. According to these characteristics, the infarct focus might be reduced and the neurological function of patients with ischemic injury might be improved [20,21]. Based on results of TUNEL staining, we found a significant increase in TUNEL-positive cells in the ischemic side of the rats' cortex when compared the MCAO group with the sham group ($p < 0.01$), indicating that neuronal apoptosis had occurred in the injured cortex after MCAO modeling. GLGZD treatment acted an effective inhibition on ischemic apoptosis of cerebral cortical neurons in the ischemia injury rats, which can ameliorate the pathological state of injured neurons and inhibited infarct expansion.

The ER is a subcellular organelle composed of a continuous membrane. The ER is a multifunctional organelle involved in various physiological activities. It is critical for maintaining intracellular homeostasis, especially in intracellular protein synthesis, calcium storage [22]. The ER is well-developed and abundant in neurons. However, the pathological changes in the ER after cerebral ischemia-reperfusion injury led to ER dysfunction, namely ERS, which leads to the dysfunction in synthesis, modification and folding of protein in the ER. The inactive proteins were largely accumulated in the ER lumen as a result. Therefore, the normal physiological activities of cells are affected, eventually leading to apoptosis [23]. Ultrastructural observations of the cells in the MCAO rats' ischemic cortex using TEM showed that the number of rough ER decreased significantly. The structure altered, with expansion, swelling, and vacuolization appeared. After GLGZD administration for 7 days, the pathological state of the rough ER in the ischemic cerebral cortex was significantly ameliorated.

Previous researchers have investigated that oxidative stress and intracellular Ca^{2+} overload are the main mechanisms of neuronal apoptosis after cerebral ischemia-reperfusion injury [24,25]. The ER is not only the major intracellular storage for Ca^{2+} in cells, but also one of the major targets of ROS attack [26]. The ER in neurons is highly developed, suggesting that the ER is a key link in the apoptotic neurocyte cascade. The apoptotic pathway induced by ER stress is one of three intracellular apoptotic signaling pathways. Studies have shown high amounts of ROS production in ischemic cells, which increases the number of oxidized phospholipids in the ER membrane. In addition, the synthesis of proteins can be interrupted by ROS, because the production of ROS induces the oxidation of sulfhydryl groups in newly generated proteins, which may become cross-linked and lose their biological activities. The accumulation of misfolded and unfolded proteins in the ER lumen finally activated ER stress (through the UPR) [27].

The Ca^{2+} pump in the ER is very sensitive to ROS levels, and the depletion of Ca^{2+} in the ER influenced the ROS-mediated regulation of Ca^{2+} in intracellular stores [28]. IP3R and SERCA are the main channel proteins associated with the Ca^{2+} pool in the ER. The Ca^{2+} reuptaked in the ER was rely on SERCA2α. IP3Rs, therefore, have the dual role of releasing Ca^{2+} and promoting the dynamic equilibrium of calcium [29]. ROS accumulation is induced by cerebral ischemia-reperfusion injury, and increased ROS levels lead to the peroxidation of membrane lipids. The membrane structure of cells is destroyed, Ca^{2+} enters the cell, IP3R in the ER membrane is activated, and SERCA is inhibited. Therefore, Ca^{2+} in the ER is excreted or reuptake of Ca^{2+} is blocked, depleting the Ca^{2+} content in the ER and causing ER dysfunction [30,31].

Our results obtained through staining with the fluorescence probe showed that the Ca^{2+} concentration and ROS levels significantly increased in the cortex cells of the MCAO-injured rats ($p < 0.01$). In addition, the measured expression of the IP3R and SERCA 2α proteins showed: the nucleus and cytoplasm IP3R expression was increased ($p < 0.01$) in the MCAO-injured cortex of the rats; the total SERCA2α protein expression level was decreased significantly ($p < 0.01$). These results support the idea that the ER released Ca^{2+} was significantly increased in the area of injured cortex after MCAO, which additionally inhibited the reuptake of Ca^{2+}. GLGZD treatment significantly reduced the ROS level and decreased the Ca^{2+} concentration in the ischemic cerebral cortex cells in the

rats. Furthermore, the significant reduction of the IP3R protein and the increase of SERCA2α ($p < 0.05$, $p < 0.01$) indicated that GLGZD effectively alleviated oxidative stress-induced injury in the neurons. After GLGZD administration, the expression of the proteins IP3R and SERCA2 was modulated, inhibiting the ER release Ca^{2+} and promoting the reuptake of Ca^{2+}, so as to facilitate a dynamic Ca^{2+} balance, which effectively alleviated ER dysfunction and reduced ERS.

The accumulation of unfolded proteins is a major manifestation of ERS. When excessive external stimulation disrupts the functions of the ER, ERS induces misfolding or unfolding of proteins. The acceleration of ERS and activation of the UPR was following the proteins accumulated in the ER lumen. The UPR is both a trigger of ERS and a key prosurvival process of ERS. The GRP78/PERK/ATF4 signaling is the main pathway regulating the protein balance and Ca^{2+} balance during the UPR [8].

PERK is a type I transmembrane protein in the ER, which has an N-terminal region with endonuclease activity, and this region detects and targets signals emitted by the ERS. The C-terminus of PERK is located in the cytoplasm and has a self-phosphorylation site. Under normal physiological conditions, the molecular chaperone of GRP78 binds PERK in a complex, which is in a low activity state. Once ERS occurs, the unfolded proteins accumulated in the ER lumen competed with PERK in binding to GRP78. It results in the complex of GRP78 and PERK uncoupled. This uncoupling causes GRP78 to be activated, and proteins are expressed in large quantities [32]. Therefore, the upregulation of GRP78 expression is regarded as a marker of ERS. In this research, both Western blotting and immunofluorescence staining were used to determine the protein level of GRP78. It was observed that the cytoplasm mainly expressed protein GRP78 was obviously more in the ischemic cortex of the MCAO group than the sham group ($p < 0.01$), indicating that ERS is involved in cerebral apoptosis induced by ischemia-reperfusion injury. Additionally, GLGZD administration significantly reduced the level of the GRP78 protein in the cytoplasm ($p < 0.05$, $p < 0.01$). Based on observations and evaluations made during the study, it was suggested that the regulation of GLGZD on neuronal apoptosis followed ischemical reperfusion injury were related to the inhibition of ERS.

PERK is the initiator protein of UPR, that is to say the UPR signal transduction is mainly mediated by PERK. Under basal conditions, the active site of PERK is sheltered by GRP78 and inhibited. Under ER stress conditions, degradation of the GRP78-PERK complex releases PERK and exposes the dimerization site, which promotes the auto-phosphorylation and dimerization of PERK, leading to the downstream target protein eukaryotic translation initiation factor 2a (eIF2a) aggregated and phosphorylated at serine 51 [33]. The affinity with the guanine nucleotide exchange factor eIF2β increased after eIF2α was phosphorylated, which inhibits the eIF2β transform from the GDP-bound to the active GTP-bound form. Thus, the proteins synthesis capability of the ER is reduced, and the levels of newly synthesized proteins decrease, and the state of ERS will be relieved [34,35]. Therefore, eIF2α is the key monitor of protein synthesis and the main target for ER to regulate its own load upon harmful stimulation. However, this protective mechanism only exists in the early stage of stress. Our results showed that ischemic injury significantly increased the protein level of PERK and the phosphorylation of eIF2α in the rat cortex of the MCAO modeling ($p < 0.05$, $p < 0.01$), and GLGZD significantly reduced the level of PERK and eIF2α. The experimental results indicated that GLGZD treatment inhibited the UPR signal transduction pathway and reduced the UPR.

Phosphorylation of eIF2α inhibited the synthesis of most proteins. Upon ERS, ribosomes access the open reading frame in the 5 noncoding regions of ATF4, which improve the translation efficiency of ATF4 and increase its expression [36]. Overexpressed ATF4 bind to the amino acid response element of the C/EBP homology protein (CHOP) after its translocation to the nucleus, promoted the synthesis of CHOP [37]. CHOP, a transcription factor played a specific and important role in ERS, is involved in the apoptosis cascade. It is an important intermediate signaling molecule [38]. Upon the stimulation of cerebral ischemia signaling, the UPR signal transduction pathway is overactivated, which mainly leads to the downstream apoptosis signaling pathway actived in the later stage of ERS.

The mechanisms of CHOP mediate apoptosis are complicated. A study of an *in vitro* ERS model showed that Ero-1α expression was controlled by CHOP. Once Ero-1α was knocked out with short interfering RNA (siRNA) technology, apoptosis induced by the ER pathway was inhibited [39]. CHOP regulated the expression of Ero-1α, which activated IP3R-related Ca^{2+} channels and the oxidative stress signaling pathway. Ca^{2+} depletion was aggravated, and ROS accumulated in the ER. These events ultimately lead to cell death [40,41]. In addition, Bcl-2 is another important target downstream of CHOP. It was reported that the Caspase-3 was subsequently activated when Bcl-2 was suppressed, leading to apoptosis [42]. All of these results suggested that CHOP influences downstream apoptosis signal transduction by its regulation on Ero-1α and Bcl-2 expression. The aggravated oxidative stress-induced injury and overload of intracellular Ca^{2+} was participated in the form of apoptosis. A multidomain apoptosis-antagonizing protein, the antiapoptotic Bcl-2 protein, forms the complex with the multidomain proapoptotic protein Bax. Specifically, Bcl-2 inhibits the activity of Bax, and Bcl-2 and Bax jointly regulate apoptosis. Therefore, we detected the aforementioned proteins using Western blotting. The total protein levels of ATF4, CHOP, Ero-1α, Bax, cleaved Caspase-3 and the nucleoprotein ATF4 were significantly increased, and the level

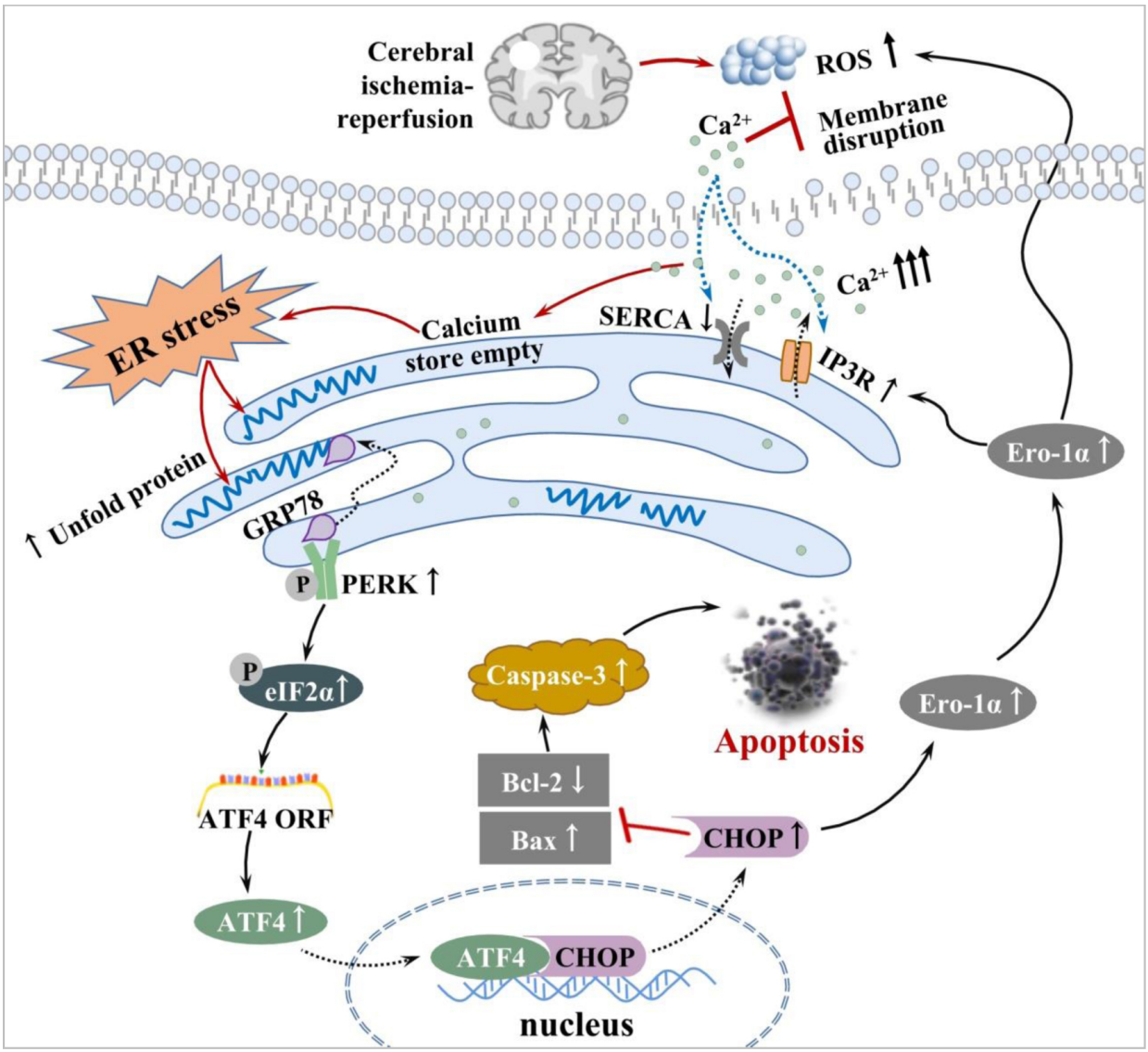

Fig. 10. The underlying mechanisms by which GLGZD attenuates apoptosis by inhibiting ERS after MCAO. Schematic diagram illustrating the involvement of the GRP78/PERK/ATF4 signaling pathway in the effects of GLGZD on ERS-induced apoptosis in the MCAO model.

of Bcl-2 was significantly decreased in the ischemic cortex in the MCAO-injured rats ($p < 0.05$, $p < 0.01$). Thus, the CHOP signal transduction pathway is activated by cerebral ischemia-reperfusion injury, and further aggravated by oxidative stress-induced injury and intracellular Ca^{2+} overload, ultimately inducing cell apoptosis. GLGZD treatment inhibited ATF4 protein synthesis and reduced its translocation to the nucleus. This process regulated CHOP signal transduction ($p < 0.05$, $p < 0.01$), reduced the degree of oxidative stress-induced injury and intracellular Ca^{2+} overload, and inhibited apoptosis.

5. Conclusions

To sum up that GLGZD significantly decreased the cerebral infarct volume in ischemic brain, ameliorated the pathological damage of cerebral ischemia-reperfusion injury on cortical neurons, improved neurological and motor functions after ischemia injury, and promoted the restoration of the quantity and morphology of the rough ER in cells of the ischemic side of the cortex. GLGZD reduced the ischemic cortex cells apoptosis, promoted the recovery of nerve and alleviated limb spasticity after cerebral ischemia injury. The protection of GLGZD turned out to be closely related to the modulation on the expression and translocation of proteins in the GRP78/PERK/ATF4 pathway (Fig. 10). GLGZD acted as an effective neuroprotective agent through the reduction of oxidative stress-induced injury and the promotion in a dynamic balance of Ca^{2+} levels, inhibiting ERS in ischemic cortical neurons and suppressing ischemia-induced neuronal apoptosis.

Abbreviations

MCAO, Middle cerebral artery occlusion; GLGZD, Gualou-Guizhi Decoction; GRP78, Glucose-regulated protein 78; ER, Endoplasmic reticulum; ERS, Endoplasmic reticulum stress; UPR, Unfolded protein response; PERK, Protein kinase R (PKR)-like ER kinase; Ero-1α, Endoplasmic reticulum oxide 1; IP3R, Inositol-1,.4,5-triphosphatereceptor; SERCA2α, Sarcoplasmic/endoplasma Ca^{2+} ATPase; eIF2α, Eukaryotic translation initiation factor 2α; ATF4, Activating transcription factor 4; CHOP, C/EBP homologous protein; Bcl-2, B-cell leukemia/lymphoma gene 2; Caspase-3, Cysteinyl aspartate specific proteinase 3; TTC, 2,3,5-triphenylte-trazolium chloride; TUNEL, TdT-mediated adenine di-nucleotide; ROS, Reactive oxygen species.

Author Contributions

LN and MH supervised the work; YChen and ZC designed the experiments and wrote the manuscript; YCao and WC performed the experiments; WX and WL provided help and advice on conception; YZ analyzed the data and reviewed the manuscript. All authors discussed the results and commented on the manuscript. All authors provided critical comments on the manuscript. All authors read and approved the final manuscript.

Ethics Approval and Consent to Participate

This study was approved by the Ethics Committee of Fujian University of Traditional Chinese Medicine (Fuzhou, China), the ethic approval number is: FJTCM IACUC 2021086.

Acknowledgment

Not applicable.

Funding

This study was funded by the National Natural Science Foundation of China [grant number 81873031], the Science Foundation of the Fujian Province, China [grant number 2021J01926], and the School Fund of Fujian University of Traditional Chinese Medicine [grant number X 2019007].

Conflict of Interest

The authors declare no conflict of interest.

References

[1] Majid A. Neuroprotection in stroke: past, present, and future. ISRN Neurology. 2014; 2014: 515716.

[2] Previch LE, Ma L, Wright JC, Singh S, Geng X, Ding Y. Progress in AQP Research and New Developments in Therapeutic Approaches to Ischemic and Hemorrhagic Stroke. International Journal of Molecular Sciences. 2016; 17: 1146.

[3] Committee of Antiaging CIAFTCMaP. Application Guidelines for Assisting stroke rehabilitation with Physical Technology. International Journal of Biomedical Engineering. 2019; 42: 100–108.

[4] Uzdensky AB. Apoptosis regulation in the penumbra after ischemic stroke: expression of pro- and antiapoptotic proteins. Apoptosis. 2019; 24: 687–702.

[5] Fu X, Cui J, Meng X, Jiang P, Zheng Q, Zhao W, *et al*. Endoplasmic reticulum stress, cell death and tumor: Association between endoplasmic reticulum stress and the apoptosis pathway in tumors (Review). Oncology Reports. 2021; 45: 801–808.

[6] Perri ER, Thomas CJ, Parakh S, Spencer DM, Atkin JD. The Unfolded Protein Response and the Role of Protein Disulfide Isomerase in Neurodegeneration. Frontiers in Cell and Developmental Biology. 2016; 3: 80.

[7] Oakes SA, Papa FR. The Role of Endoplasmic Reticulum Stress in Human Pathology. Annual Review of Pathology: Mechanisms of Disease. 2015; 10: 173–194.

[8] Qian Z, Zhu L, Li Y, Li Y, Wu Y, Fu S, *et al*. Icarrin prevents cardiomyocyte apoptosis in spontaneously hypertensive rats by inhibiting endoplasmic reticulum stress pathways. Journal of Pharmacy and Pharmacology. 2021; 73: 1023–1032.

[9] Chen Y, Chen L, Tao J. Clinical research on treating limbs spasm from cerebral apoplexy with the Gualou Guizhi decoction. Clinical Journal of Chinese Medicine. 2013; 5: 7–9.

[10] Li Z. Effect evaluation of Gualou Guizhi Decoction in the treatment of lower limb spasticity after stroke. Chinese Journal of Modern Drug Application. 2020; 14: 205–207.

[11] Wang J, Xia X, Jiang S. Linical Observation of Gualou Guizhi Tang for Lower Limb Spasm After Stroke and Its Effect on Motor Function of Lower Limbs. Journal of New Chinese Medicine. 2020; 52: 28–31.

[12] Nan L, Yang L, Zheng Y, He Y, Xie Q, Chen Z, *et al*. Effects of Gualou Guizhi Decoction Aqueous Extract on Axonal Regeneration in Organotypic Cortical Slice Culture after Oxygen-Glucose Deprivation. Evidence-Based Complementary and Alternative Medicine. 2017; 2017: 5170538.

[13] Nan L, Xie Q, Chen Z, Zhang Y, Chen Y, Li H, *et al*. Involvement of PARP-1/AIF Signaling Pathway in Protective Effects of Gualou Guizhi Decoction against Ischemia–Reperfusion Injury-Induced Apoptosis. Neurochemical Research. 2020; 45: 278–294.

[14] Zhan C, Yang J. Protective effects of isoliquiritigenin in transient middle cerebral artery occlusion-induced focal cerebral ischemia in rats. Pharmacological Research. 2006; 53: 303–309.

[15] Longa E. Reversible middle cerebral artery occlusion without craniotomy in rats. Stroke. 1989; 20: 84–91.

[16] Ashworth B. Preliminary trial of carioproda in multiple sclerosis. Practitioner. 1964; 192: 540–542.

[17] LEE S, HONG Y, PARK S, LEE S, CHANG K, HONG Y. Comparison of Surgical Methods of Transient Middle Cerebral Artery Occlusion between Rats and Mice. Journal of Veterinary Medical Science. 2014; 76: 1555–1561.

[18] Rong W, Yang L, Li CY, Wu XT, Zhou ZD, Zhu WL, *et al*. MiR-29 inhibits neuronal apoptosis in rats with cerebral infarction through regulating Akt signaling pathway. European Review for Medical and Pharmacological Sciences. 2020; 24: 843–850.

[19] Mao R, Zong N, Hu Y, Chen Y, Xu Y. Neuronal Death Mechanisms and Therapeutic Strategy in Ischemic Stroke. Neuroscience Bulletin. 2022. (in press)

[20] Wang J, Zhong W, Su H, Xu J, Yang D, Liu X, *et al*. Histone Methyltransferase Dot1L Contributes to RIPK1 Kinase-Dependent Apoptosis in Cerebral Ischemia/Reperfusion. Journal of the American Heart Association. 2021; 10: e022791.

[21] Fricker M, Tolkovsky AM, Borutaite V, Coleman M, Brown GC. Neuronal Cell Death. Physiological Reviews. 2018; 98: 813–880.

[22] Go BS, Kim J, Yang JH, Choe ES. Psychostimulant-Induced En-

doplasmic Reticulum Stress and Neurodegeneration. Molecular Neurobiology. 2017; 54: 4041–4048.
[23] Iurlaro R, Munoz-Pinedo C. Cell death induced by endoplasmic reticulum stress. FEBS Journal. 2016; 283: 2640–2652.
[24] Narne P, Pandey V, Phanithi PB. Interplay between mitochondrial metabolism and oxidative stress in ischemic stroke: An epigenetic connection. Molecular and Cellular Neurosciences. 2017; 82: 176–194.
[25] Hu J, Pang WS, Han J, Zhang K, Zhang JZ, Chen LD. Gualou Guizhi decoction reverses brain damage with cerebral ischemic stroke, multi-component directed multi-target to screen calcium-overload inhibitors using combination of molecular docking and protein-protein docking. Journal of Enzyme Inhibition and Medicinal Chemistry. 2018; 33: 115–125.
[26] Bahar E, Kim H, Yoon H. ER Stress-Mediated Signaling: Action Potential and Ca(2+) as Key Players. International Journal of Molecular Sciences. 2016; 17: 1558.
[27] DeGracia DJ, Kumar R, Owen CR, Krause GS, White BC. Molecular Pathways of Protein Synthesis Inhibition during Brain Reperfusion: Implications for Neuronal Survival or Death. Journal of Cerebral Blood Flow and Metabolism. 2002; 22: 127–141.
[28] Tu BP, Weissman JS. Oxidative protein folding in eukaryotes: mechanisms and consequences. Journal of Cell Biology. 2004; 164: 341–346.
[29] Shah SZA, Zhao D, Khan SH, Yang L. Regulatory Mechanisms of Endoplasmic Reticulum Resident IP3 Receptors. Journal of Molecular Neuroscience. 2015; 56: 938–948.
[30] Gleichmann M, Mattson MP. Neuronal Calcium Homeostasis and Dysregulation. Antioxidants and Redox Signaling. 2011; 14: 1261–1273.
[31] Vervloessem T, Yule DI, Bultynck G, Parys JB. The type 2 inositol 1,4,5-trisphosphate receptor, emerging functions for an intriguing Ca2+-release channel. Biochimica et Biophysica Acta (BBA) - Molecular Cell Research. 2015; 1853: 1992–2005.
[32] Ye Z, Wang N, Xia P, Wang E, Liao J, Guo Q. Parecoxib suppresses CHOP and Foxo1 nuclear translocation, but increases GRP78 levels in a rat model of focal ischemia. Neurochemical Research. 2013; 38: 686–693.
[33] McQuiston A, Diehl JA. Recent insights into PERK-dependent signaling from the stressed endoplasmic reticulum. F1000Research. 2017; 6: 1897.
[34] Joshi M, Kulkarni A, Pal JK. Small molecule modulators of eukaryotic initiation factor 2alpha kinases, the key regulators of protein synthesis. Biochimie. 2013; 95: 1980–1990.
[35] Bellato HM, Hajj GN. Translational control by eIF2alpha in neurons: Beyond the stress response. Cytoskeleton. 2016; 73: 551–565.
[36] Rasheva VI, Domingos PM. Cellular responses to endoplasmic reticulum stress and apoptosis. Apoptosis. 2009; 14: 996–1007.
[37] Yaman I, Fernandez J, Liu H, Caprara M, Komar AA, Koromilas AE, *et al*. The Zipper Model of Translational Control: A Small Upstream ORF Is the Switch that Controls Structural Remodeling of an mRNA Leader. Cell. 2003; 113: 519–531.
[38] Hosoi T, Ozawa K. Endoplasmic reticulum stress in disease: mechanisms and therapeutic opportunities. Clinical Science. 2009; 118: 19–29.
[39] Kooptiwut S, Mahawong P, Hanchang W, Semprasert N, Kaewin S, Limjindaporn T, *et al*. Estrogen reduces endoplasmic reticulum stress to protect against glucotoxicity induced-pancreatic beta-cell death. Journal of Steroid Biochemistry and Molecular Biology. 2014; 139: 25–32.
[40] Li G, Mongillo M, Chin KT, Harding H, Ron D, Marks AR, *et al*. Role of ERO1-alpha-mediated stimulation of inositol 1,4,5-triphosphate receptor activity in endoplasmic reticulum stress-induced apoptosis. Journal of Cell Biology. 2009; 186: 783–792.
[41] Zito E. ERO1: A protein disulfide oxidase and H2O2 producer. Free Radical Biology and Medicine. 2015; 83: 299–304.
[42] Kureel J, John AA, Raghuvanshi A, Awasthi P, Goel A, Singh D. Identification of GRP78 as a molecular target of medicarpin in osteoblast cells by proteomics. Molecular and Cellular Biochemistry. 2016; 418: 71–80.